Histidine-containing amphiphilic peptide-based non-cytotoxic hydrogelator with antibacterial activity and sustainable drug release

Article

Accepted Version

Hansda, B., Majumder, J., Mondal, B., Chatterjee, A., Das, S., Kumar, S., Gachhui, R., Castelletto, V. ORCID: https://orcid.org/0000-0002-3705-0162, Hamley, I. W. ORCID: https://orcid.org/0000-0002-4549-0926, Sen, P. ORCID: https://orcid.org/0000-0002-1233-1822 and Banerjee, A. ORCID: https://orcid.org/0000-0002-1309-921X (2023)

It is advisable to refer to the publisher's version if you intend to cite from the work. See Guidance on citing.

www.reading.ac.uk/centaur

CentAUR

Central Archive at the University of Reading

Reading's research outputs online

Histidine- Containing Amphiphilic Peptide- Based Non-cytotoxic Hydrogelator with Antibacterial Activity and Sustainable Drug Release

Biswanath Hansda,[a] Jhilam Majumder,[b] Biplab Mondal,[a] Subhadeep Das,[c] Sourav Kumar,[d] Ratan Gachhui,[b] Valeria Castelletto[e], Ian W. Hamley,[e] and Arindam Banerjee[a]*

Abstract:

A histidine based amphiphilic peptide (**P**) has been found to form an injectable transparent hydrogel in phosphate buffer solution (PBS) over a pH range from 7.0 to 8.5 with an inherent antibacterial property. It also formed a hydrogel in water at pH = 6.7. The peptide self-assembles into a nanofibrillar network structure which is characterized by high-resolution transmission electron microscopy (HR-TEM), field-emission scanning electron microscopy (FE-SEM), atomic force microscopy (AFM), small-angle X-ray scattering (SAXS), Fourier transform infrared (FT-IR) spectroscopy, and wide-angle powder X-ray diffraction (PXRD). The hydrogel exhibits efficient antibacterial activity against both Gram-positive bacteria *Staphylococcus aureus* (*S. aureus*) and Gram-negative bacteria *Escherichia coli* (*E. coli*). The minimum inhibitory concentration of the hydrogel ranges from 20 to 100 µg/ml. The hydrogel is capable of encapsulation of the drugs Naproxen, a nonsteroidal anti-inflammatory drug (NSAID) and Doxorubicin, an anticancer drug, but selectively and sustainably the gel releases only Naproxen, 84% being released in 84 h. The hydrogel is biocompatible with HEK 293T cells, and can thus has potential as an potent antibacterial and drug releasing agent. Another remarkable feature of this hydrogel is its magnification property like a convex lens.

Introduction:

For decades, gradual overuse and misuse of antibiotics has created a window for bacteria to grow resistance to conventional antibiotics. [1-2] Like others man-made and natural disasters, drug resistant microbes have become a great threat not only to the human beings but also to animals, agriculture and the environment. [3-4] The World Health Organization (WHO) has reported on the threat from microbial resistance to antibiotics. The report shows that many people from all over the worldare suffering infections caused by bacterial resistance which leads to the death of about 700,000 people per year. Projected death, as estimated by some experts, will reach up to 10 million in the next three decades if innovative and effective antibiotics are not discovered to solve the problem. [5] To combat the problem WHO was asked by its member states in 2016 to construct a priority list of bacterial resistance to antibiotics for supporting related research and developing effective antibacterial drugs in the following years. [6,7] So it is a great challenge to scientists and researchers all over the world to develop new effective therapeutics to overcome the challenge of antimicrobial resistance. However, with the progress of therapeutic research, it is necessary to improve the appropriate vehicle to deliver a drug to the proper target. [8,9] Though there are many complicated proposed drug delivery systems, several ways of transportation of drug have been studied. These include peptide based hydrogels, DNA aptamers, liposomes, different types of polymers, oligomers, nanoparticles etc. [10] The burst release of drug is a major disadvantage for the a drug delivery system because this process causes a high local concentration of drug. An acceptable drug delivery system should show sustained and controllable release of drug. [11]

Over the last few decades, low molecular weight supramolecular hydrogelators [12-13] have emerged as promising systems with versatile applications as soft materials. [14,15] Supramolecular

hydrogelators immobilize the movement of water molecules trapped within the three dimensional network structure which is formed by the hierarchical assembly[16] of gelator molecules and stabilized by various non-covalent interactions including hydrogen bonding, hydrophobic interactions, van der Waals interactions, π-π interactions, cation-π interactions, charge transfer interactions etc.[17] This kind of soft material being easily usable, nontoxic, biocompatible, and biodegradable has extensive applications in biomedical technology as well as in environmental science. The tunable property of hydrogel through various stimuli such as pH, mechano-responsiveness, chemo-responsiveness, light, heat, and others make them suitable as carriers of numerous drugs and biomolecules.[18-19] Confinement of a large volume of water into 3D network of hydrogel enables them to mimic biological system and thus to be used in tissue engineering[20,21], cell culture[22-23], tissue regeneration[24], as antibacterials[25,26], and in wound healing[27] or cell adhesion and proliferation.[28,29] Hydrogels also have potential as environmental remedients by removing toxic organic dyes[30] heavy metals[30-31] and oils (oil spill recovery).[30,32-33] Apart from this, a notable property of hydrogel is its thixotropic[28,34,35] nature in which a gel-sol-gel transition occurs. By applying a mechanical shear strain/stress a gel can be broken and turned into solution and this can reform when the applied force is withdrawn. In recent years, this property has been explored to make injectable hydrogels that can be used in localized therapy in a particular tissue [36]

In recent years, peptide-based hydrogels[37,38] have been developed as biomaterials that act as antimicrobial agents[39] for the treatment of infectious diseases.[40]. Several kinds of hydrogels have been reported so far,[41-42] but there are few peptide- based low molecular weight hydrogels that inherently show antimicrobial activity.[43] Polycationmoieties have antimicrobial properties but often show a certain level of toxicity to mammalian cells.[44] Thus recently, peptide-based low

molecular weight hydrogels have drawn attention as antimicrobial agents in the field of therapeutics.

In this context, the present study reports the hydrogelation of N-Boc protected peptide-based amphiphile (**P**) by various supramolecular interactions in physiological phosphate buffer at pH 7.46. Furthermore, the thixotropic nature of the hydrogel, **P**, has also been investigated. The antibacterial properties of the hydrogel are studied, and it has been found that it shows antibacterial activity against Gram-positive bacteria, *Staphylococcus aureus* (*S. aureus*), as well as Gram-negative bacteria *Escherichia coli* (*E. coli*). Moreover, the hydrogel as a soft material has been employed to encapsulate the anticancer drug Naproxen, and it is shown to release the drug slowly in vitro for 84 h under physiological condition at pH 7.46 and temperature 37 °C. In this case, the drug is intact after release as shown by the absorbance of Naproxen. For practical applicability, the hydrogel is non-cytotoxic to HEK-293T cells at its minimum inhibitory concentration (MIC) and shows negligible cytotoxicity at higher concentrations. This work may be considered as a unique one that lies in the fact that the hydrogel shows simultaneously antibacterial activity and a sustained drug release capacity based on a simple peptide-based molecule. The lack of cytotoxicity, injectability, antibacterial activity against Gram- positive and Gram- negative bacteria and release of drug at physiological pH and temperature makes this peptide- based biomaterial a good candidate for antibacterial treatment and as a drug delivery vehicle in future. Moreover, this peptide- based hydrogel shows an interesting property of magnifying images and text if viewed through the hydrogel. These remarkable properties suggest multipurpose applications in future for this gel- based biomaterial.

EXPERIMENTAL SECTION

Materials:11-aminoundecanoic acid, L-valine and L-histidine were purchased from Sigma Aldrich. Thionyl chloride, MeOH, NaOH, chloroform, DMF, formic acid, ethyl acetate, DCC, hydroxybenzotriazole (HOBt), silica gel (100−200 mesh), and petroleum ether were purchased from SRL (India). Here milli-Q water and phosphate buffer were used in all experiments. Gram-negative *Escherichia coli* ATCC 25922 and Gram- positive *Staphylococcus aureus* ATCC 25923 were used. All the microorganisms were cultured and maintained in Luria–Bertani medium. Cell studies also used MTT (Himedia, India), DMEM media (Himedia, India), FBS (FBS; Gibco, USA), and DMSO (Merck, India). Human embryonic kidney (HEK-293) cells were obtained from the national Centre for Cell Science (NCCS), Pune. The cells were grown in DMEM medium (Himedia, India) supplemented with 2 mM l-glutamine, 10% fetal bovine serum (FBS; Gibco, USA), 1% penicillin-streptomycin, under a 5% CO_2 atmosphere at 37 °C.

Peptides Synthesis and Their Characterization: All the peptides are synthesized by standard solution phase methods using racemization- free reagents. The detailed synthetic procedures are provided in the Supporting Information. All the peptides were fully characterized by ^1H NMR spectroscopy, mass spectrometry, and ^{13}C NMR spectroscopy. All NMR data were recorded on a Bruker DPX 500 MHz or Bruker DPX 400 MHz spectrometer at 300 K. Concentrations was in the range of 5 to10 mmol in $CDCl_3$ or DMSO-d_6. Electrospray-ionization mass spectra (ESI-MS) were obtained using a Q-Tofmicro (Waters Corporation) mass spectrometer.

Morphological Imaging: The morphological features of hydrogel was evaluated using field emission scanning electron microscopy (FE-SEM, JEOL-JSM-7500F), atomic force microscopy (AFM, Auto probe CP Base Unit di CP-II instrument, Model AP-0100), and high resolution transmission electron microscopy (HR-TEM, JEOL electron microscope at an accelerating

voltage of 200 kV). For the FE-SEM and AFM the samples were prepared by drop casting 20 µl of gel sample (0.002% w/v) on mica foil. Samples for HR-TEM was prepared by drop- casting 10 µl aliquots on TEM grids (300 mesh Cu grids). In each case the drop- cast samples were dried under vacuum at 25 °C for 14 h. Then morphological images of the samples were obtained using the respective instruments.

FT-IR Study: A Nicolet 380 FT-IR spectrophotometer (Thermo Scientific) was used to obtain Fourier transform infrared spectra of xerogels.

PXRD Study: The powder X-ray diffraction data of the xerogel were recorded using a Rigaku SmartLab X-ray diffractometer operated at 9 kW (45 kV, 200 mA) using Ni filtered CuKα radiation and a 1D detector with scan speed 0.3 s and step size 0.02° over the range $2\theta = 10\text{-}50°$.

SAXS Study: Synchrotron SAXS experiments on solutions were performed on beamline B21 at Diamond (Didcot, UK).[1] Gel samples were loaded into PEI capillaries loaded into a gel sample cell.[2] Data was collected at 20 °C. The sample detector distance was 3.71 m and the wavelength was 0.95 Å. The images were captured using a Pilatus 1M detector. Data processing (background subtraction, radial averaging) was performed using dedicated beamline software (ScÅtter).

General Procedure for Antibacterial Study: Antibacterial activity was tested against Gram-positive bacteria (*Staphylococcus aureus*) and Gram-negative bacteria (*Escherichia coli*) in vitro using a well-plate diffusion assay in an agar plate. The gel materials of **P** were taken as test samples and phosphate buffer was used as negative control and ampicillin (100 µg/ml) was taken as positive control.

General Procedure for bacterial imaging: Bacterial suspensions (1 mL) in Luria Broth were incubated with 50 µl (1 mg mL^{-1}) gelator for 18 hours at 37 ^{0}C then suspensions were

centrifuged at 6000 rpm for 5 minutes. The precipitates were washed with 0.85 % NaCl solution twice, then the bacterial precipitates were mixed with 2.5% glutaraldehyde in PBS and incubated at room temperature for 30 minutes then at 4 ^{0}C to fix overnight. Then the pellets were collected by centrifugation and washed with ultrapure water twice. Next, dehydration of the sample was performed in different ethanol grades (30%, 50%, 70%, 90% and 100% for 10 minutes each step). The samples were drop- cast on glass plate and images were recorded with a fField emission scanning electron microscope (FE-SEM) at 5 kV.

General Procedure for Drug Release Study: For the drug release study,hydrogels incorporating Naproxen or Doxorubicin were prepared. First, 1 ml of PBS was used as the release medium. Then, 500 μl of the release medium was taken out at different time intervals to measure the UV absorbance. Release was monitored for 72 h. For CP, release studies were done in PBS pH 7.4 to mimic the physiological milieu, while release of 5-FU was studied at both PBS pH 7.4 and 5.5 to mimic healthy and cancerous tissue environments. The release efficiency was calculated as

$$Release\ (\%) = \frac{release\ concentration}{loaded\ concentration} \times 100$$

General Procedure for Cell Viability Assay Study: Cell viability was performed using a mitochondria enzyme dependent MTT reduction assay (Mosmann, 1983). HEK-293 cells were seeded into 96 well plate at a density of 10^4 cells/well treated with different concentrations of **P** (0–250 μM) for 24 h. MTT (Himedia, India) was prepared at a concentration of 5 mg/ml in DPBS before use. A total of 100 μl of MTT (0.5 mg/ml) was added to each well. The cells were incubated at 37 °C and 5% CO_2 humidity for 4 h. After incubation, the MTT solution was aspirated and 200 μl of dimethylsulfoxide (DMSO) was added to each well to sufficiently

dissolve the formazan precipitate. Cell viability was calculated by measuring absorbance at 570

nm using a microplate reader. Results were expressed as percentage of control:

$$\text{Cell Viability (\%)} = \frac{Abs.(treated) - Blank}{Abs.(Control) - Blank} \times 100$$

RESULTS AND DISCUSSION

Gelation Study and Physical Appearance of the Hydrogel: We successfully synthesized the

N-terminally Boc-protected amphiphilic peptide gelator, BUVVH-OH (**P**) (Figure 1a) and tested

for gelation in phosphate buffer. The detailed synthetic procedures for making the gelator

molecule are provided in the Supporting Information (Scheme1, S1-S3) The gelator was placed

in a clean glass vial containing 1 ml phosphate buffer solution (PBS) of physiological pH 7.46.

The resultant mixture was heated on a hot plate until a homogeneous and clear solution was

obtained which was left standing. After 10 minutes the solution turned into a gel, asconfirmed by

vial inversion. The minimum gelation concentration of the gel was found to be 2.0 mg/ml (0.20%

w/v) at physiological pH 7.46. The gelator also formed a gel in ultrapure Q water at pH 6.7, in

other phosphate buffer at pH 7.0 and 8.5. Furthermore, the physical appearance of the hydrogel

was examined with the variation of concentration, temperature and time. Figure 1b (side view)

and 1c (top view) show the hydrogel formed using 4 mg of gelator in 2 ml of phosphate buffer

that are transparent. It was observed that the gelation solution of 1.0 g/ml was very viscous in

nature and highly transparent (Figure 1d). Transparent hydrogels were formed for gelator

concentrations of 2.0 and 4.0 mg/ml. As the concentration was increased above 4.0 mg/ml the

hydrogels gradually became more opaque. Figure1e shows four hydrogels at different

concentrations (2, 4, 6 and 8mg/ml) that exhibited the alteration of physical appearance of the

hydrogels from transparent to opaque. No effect was observed varying temperature or time. It was observed that the peptide- based transparent hydrogel has a very interesting property of magnifying anything viewed through it. For example,Figure S4 (a-d) shows magnification (several times) of Bengali letters. Thus, this transparent hydrogel has lens-like property. It can be envisaged that the peptide- containing hydrogel based soft biomaterial can be used as a new soft magnifying material.
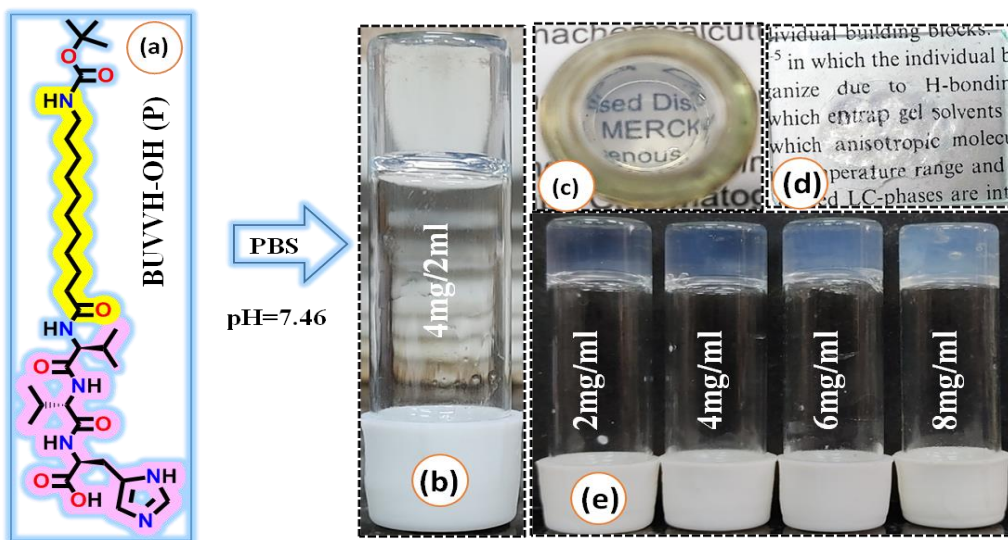
Figure 1. (a) Molecular structure of the gelator BUVVH-OH; (b) and (c) Visualization of clear transparent hydrogel in side top views respectively; (d) Very viscous solution of the gelator (1 mg/ml) showing transparency and (e) Concentration series of hydrogels showing alteration of transparency.

Morphological Analysis. Morphological analyses *i.e*. insight into structure of the hydrogel clearly revealed that the gelling ability is due to the 3D network structure comprising numerous nanofibers. This was confirmed by high resolution transmission electron microscopy (HR-TEM, Figure 2a), field emission scanning electron microscopy (FE-SEM, Figure 2b), and atomic force microscopy (AFM, Figure 2c and 2d). For each of the techniques, xerogels obtained from the freshly prepared hydrogel were imaged. These microscopic images show nanofiber networks which are presumably formed by self-assembly of the gelator via non-covalent interactions such as π-π interactions, hydrogen bonding, and van der Waals interactions. Images indicate that these fibers are not uniform over the bulk. The fibers are elongated several micrometers in length. Detailed investigation (by image J) of the AFM image showed that the nanofibers are 60 nm in width and some of the fibers are wrapped around each other to form relatively more thick aggregated fibers. Differences in HR-TEM, AFM, and FE-SEM images may be attributed to the method of preparation of samples in morphological studies. However, it is evident that nanofibers are formed and form an entangled structure with cavities that can entrap water molecules to form a self-supporting gel.
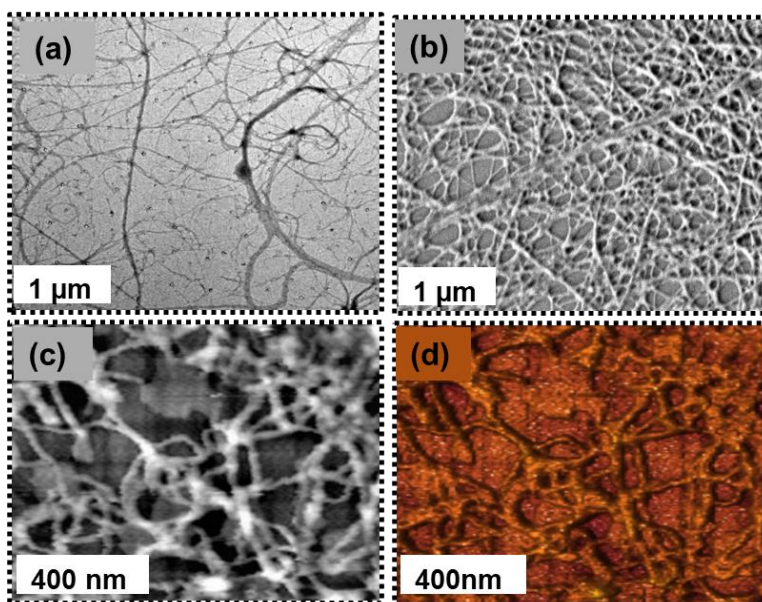
Figure 2. Images of the xerogel obtained from BUVVH-OH from (a) HR-TEM, (b) FE-SEM, (c),(d)= AFM .

FT-IR Analysis: A detailed study of Fourier transform infrared (FT-IR) spectroscopy of a xerogel was carried out to get information on non covalent interactions that provide insights into the self-assembly of of the gelator. The spectrum is shown in Figure 3 with peaks listed in Table 1. The intense peak at 3284 cm^{-1} corresponding to hydrogen bonded N–H stretching. The absorption at 2965 cm^{-1} indicates the asymmetric stretching of –CH_3 while the peaks at 2924–2852 cm^{-1} show the aliphatic C–H symmetric stretching of the –CH_2 group in the undecanoic chain). A significant C=O stretching frequency appears at 1683 cm^{-1} that corresponds to the hydrogen bonded urethane group (Boc >C=O). The strong absorption peak at 1630 cm^{-1} shows the C=O stretching of the extended amide backbone. The IR absorption band of amide N–H bend arises at 1535 cm^{-1}. Another significant peak at 1470 cm^{-1} is due to the C–H symmetric stretch, while the peaks at 1392–1365 cm^{-1} correspond to C–H asymmetric stretching (for both case Val–

Table 1: FT-IR data

CH$_3$). However, the amide carbonyl peak at 1630 cm^{-1} clearly indicates that the gelator molecules are arranged themselves into a β-sheet-like structure.

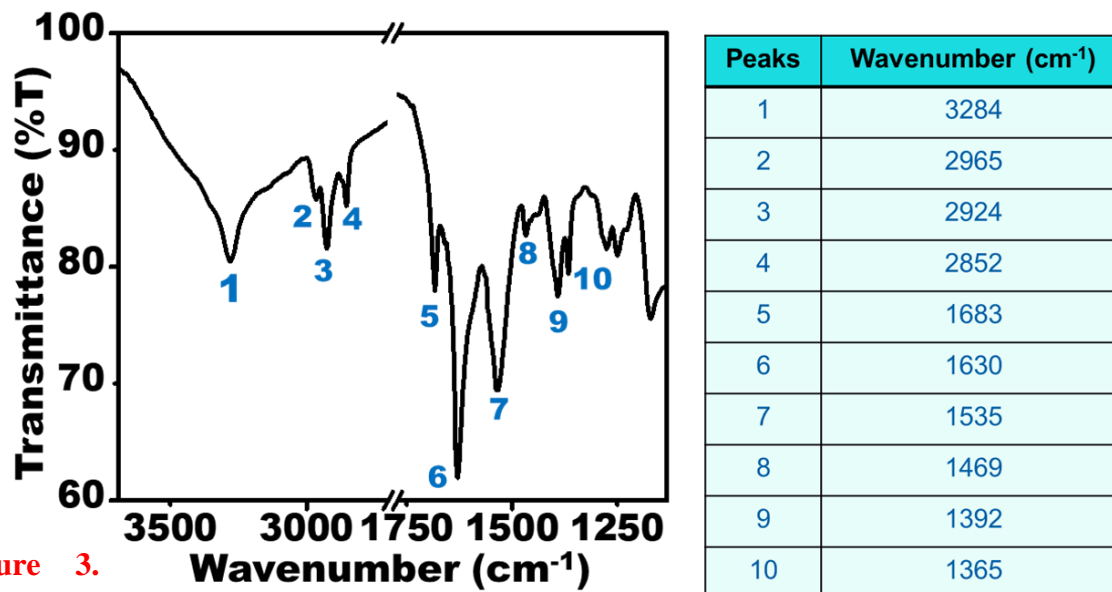| Peaks	Wavenumber (cm^{-1})
1	3284
2	2965
3	2924
4	2852
5	1683
6	1630
7	1535
8	1469
9	1392
10	1365

Figure 3. Fourier Transform infra-red spectrum from the xerogel of BUVVH-OH.

SAXS and PXRD Analysis: Small angle X-ray scattering (SAXS) was performed on a native hydrogel and powder x-ray diffraction on a xerogel to obtain insights into the gel state structure and the packing of the gelator molecules. A *d*- spacing value 49.6 Å was obtained from the SAXS intensity profile (Figure 4a). This value is smaller than
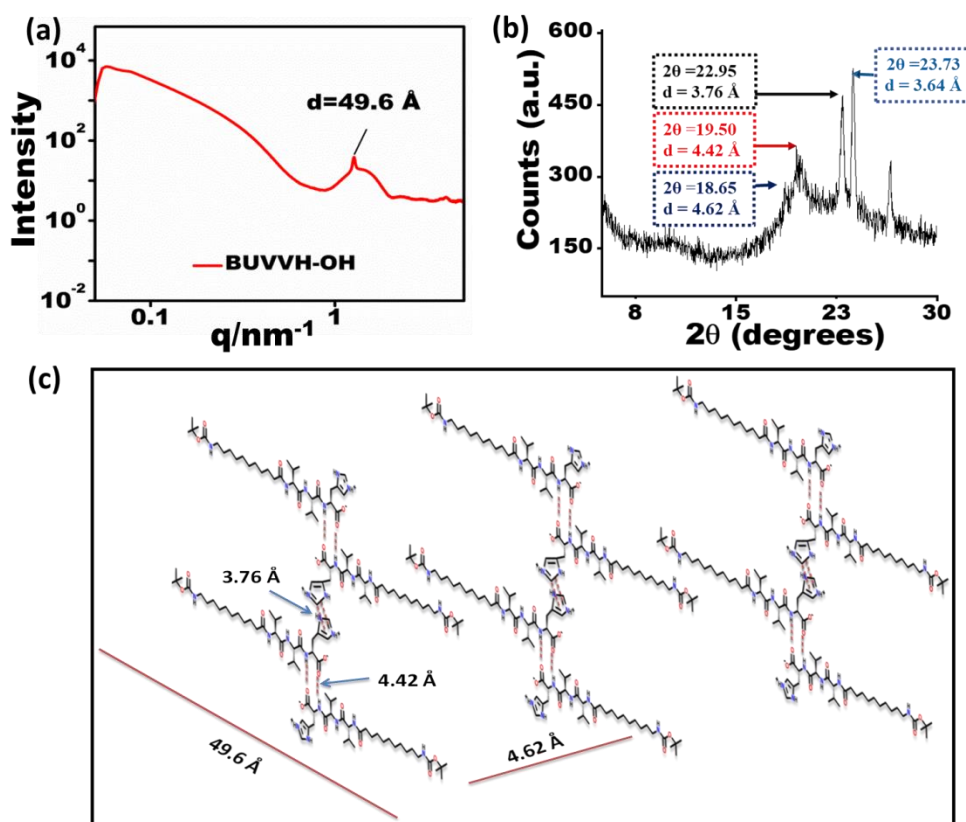
Figure 4. (a) Small angle X-ray scattering data from a hydrogel BUVVH-OH; (b) Wide angle powder X-ray diffraction (PXRD) pattern from a BUVVH-OH hydrogel; (c) Proposed schematic model for the packing arrangement of the gelator molecules based on their SAXS and PXRD data.

twice the molecular length (2×28.4 Å) but the difference is not large. The protective Boc-group at N-terminus, in the tail of the long chain may impose hindrance to interdigitation between the long chains.[45] However, the 2θ (CuKα) values evaluated from the PXRD data range from 18.65 to 33.50° (Figure 4b). The d-spacing value of 4.62 Å at $2\theta=18.65°$ corresponds to the distance between the backbones of two peptides as generally observed in the conventional β-sheet

structure. The d-spacing value of 4.42 Å at 2θ=19.50° is likely due to hydrogen bonding between two gelator molecules of the xerogel. A significant peak at 2θ=22.95° that corresponds to the d-spacing of 3.76 Å clearly suggests the presence of π-π stacking arrangement between the aromatic moieties of the gelator molecules. Combining the evidence obtained from SAXS, PXRD and FT-IR analyses, it is proposed that the gelator molecules are self-assembled in the gel state with a β-sheet-like structure stabilized by the non-covalent interactions. A tentative model for the packing of gelator molecules is shown in Figure 4c.

Rheological Study and Thermal Effect: To investigate the mechanical strength and stability of a gel, rheological measurements of the dynamic viscoelastic of hydrogel obtained from **P** were carried out. Such studies of hydrogel stability, strength and stiffness are essential for practical use of hydrogels in biomedical science. Oscillatory frequency sweep measurements of the hydrogel were performed and the storage modulus (G′) and loss modulus (G″) were measured as a function of angular frequency as presented in Figure 5a. The experiment was carried out with a gelator concentration 0.3% (w/v) at constant temperature of 27 °C keeping the strain low (in the linear viscoelastic regime) and constant at 0.1%. The measured data showed that the storage modulus (G′) of the hydrogel is higher than that of the loss modulus (G″) and mostly independent of angular frequency which reveals the presence of viscoelastic stable gel.[46] There is no cross-over of the modulus components within the angular frequency region in the experiment. Furthermore, the storage modulus (G′) in this experiment is in the order of 1.1×10^3 Pa and is one order higher than that of the loss modulus (G″). This clearly indicates that the hydrogel matrix has adequate resistance to external forces.[47] Interestingly, this peptide hydrogel also exhibited thixotropic property.
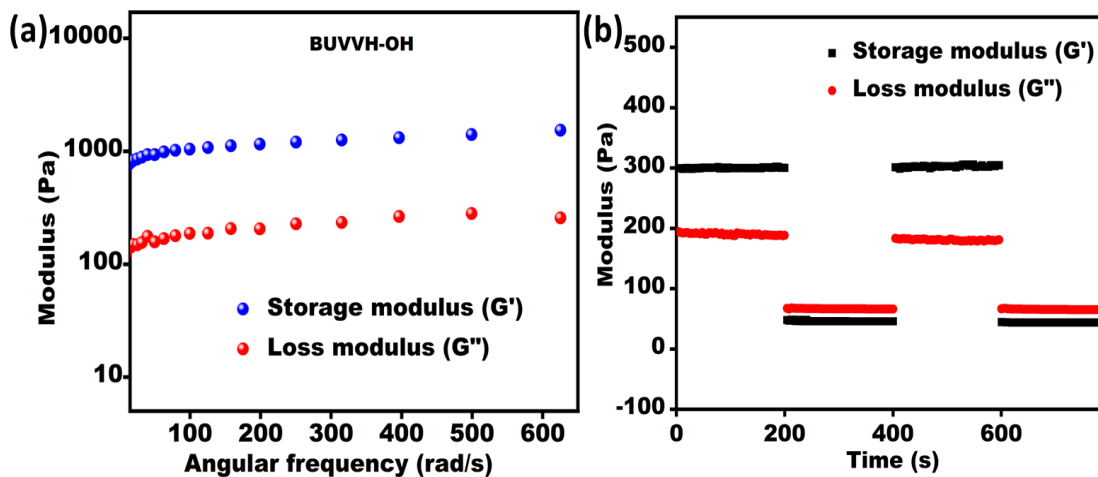
Figure 5. (a) Frequency sweep experiment of the hydrogel BUVVH-OH (0.3% (w/v) at a constant strain of 0.1%. (b) Thixotropy: Time sweep experiment (step-strain rheological analysis) of the thixotropic hydrogels BUVVH-OH at a fixed angular frequency of 1 rad/s (at 25 °C).

For this, a step-strain time dependent study was performed using 0.3% (w/v) hydrogel. The strain was continuously increased from 0.1% to 30% to break the gel matrix (Figure 5b). Then its recovery at constant strain of 0.1% was recorded with time. The storage modulus (G′) immediately falls below the loss modulus (G′) line upon application of strain. This phenomenon confirmed the transformation of the gel to a sol- like material. However, after removal of the high applied strain the storage modulus recovered to its initial value, i.e. G′ line exceeds G″. Visual evidence showing the thixotropic property of the hydrogel is shown in the supporting information in Figure S5. The effect of temperature on the hydrogel was also investigated. It was observed that the gel-to-sol transition temperatures (T_{gel}) of the hydrogel are dependent on the

concentration of the gelator. The T_{gel} of the hydrogel increases linearly with increasing gelator concentration (Figure S6).

Antibacterial Study: Microbial infections caused by implantation of biomaterials are a major challenge that requires of the development of novel smart biomaterials with inherent antimicrobial activity. To evaluate the antibacterial activity of hydrogel **P** against Gram-positive and Gram-negative bacteria agar well-plate diffusion experiments were carried out, these reveal areas of inhibition of bacterial spreading. In this experiment phosphate buffer was used as negative control whereas the hydrogel sample was used as investigative material. The investigation showed that the hydrogel was not only active against Gram-positive bacteria but also active against Gram-negative bacteria. The formation of inhibition zones was observed in the screening test which suggests that the hydrogel is active against Gram-positive *Staphylococcus aureus* (*S. aureus*) bacteria, as well as Gram-negative *Escherichia coli* (*E. coli*) bacteria (Figure 6a) at a minimal concentration of 20 µg/ml. To evaluate the MIC (minimum inhibitory concentration) value of the hydrogel the micro dilution method was used. It was observed that the growth of *E. coli* and *S. aureus* was significantly inhibited by the hydrogel. The antibacterial efficacy of the hydrogel was investigated at MIC value ranges from 20 to 100 µg/ml (Figure 6b). The hydrogel is more or less equally effective against *S. aureus* and *E. coli* at the same concentration (Figure 6c). It is notable that the MIC value of the hydrogels containing silver ions or silver nanoparticles as previously reported in literature are typically lower.[48] This can be attributed to the fact that here the hydrogel itself confers its antibacterial activity in comparison with its counterparts that contain silver ions or silver nanoparticles. The hydrogel
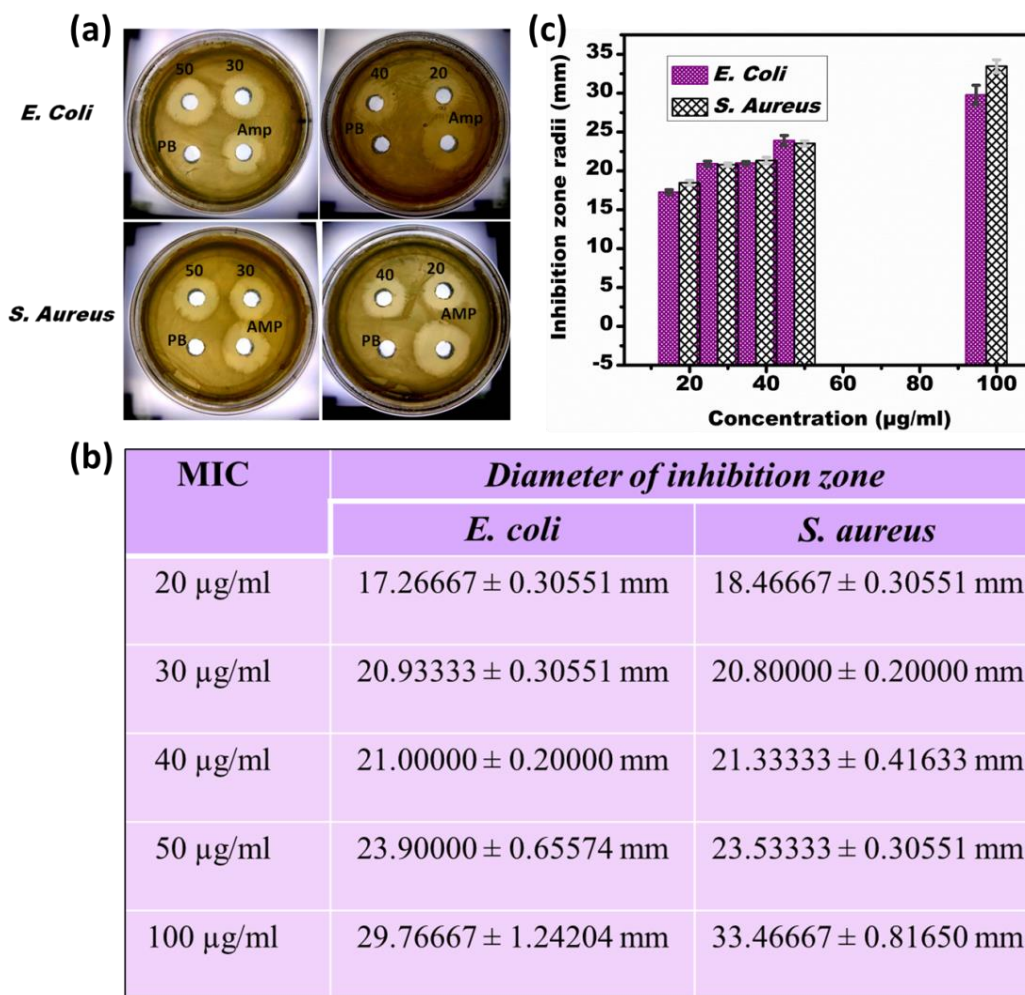
Figure 6. (a) Antibacterial efficacy of the hydrogel on Gram–negative and Gram–positive bacteria by agar-diffusion method- (i) *E. coli* (ii) *S. aureus.* (b) Minimum inhibitory concentration with diameter of inhibition zone of the respective bacteria. (c) Inhibition zone radii against concentration of the hydrogel (µg/ml).

containing silver manifests antibacterial efficacy by releasing silver ions or silver nanoparticles whereas here case the amphiphilic peptide based hydrogel of **P** exhibits inherent antibacterial

properties. Thus this hydrogel has some advantages over silver-containing hydrogels which show side effects including skin pigmentation, and inflammation due to reactive oxygen species and oxidative DNA damage.[49] , With increasing concentration of the hydrogel the inhibition zone increases accordingly, as shown in Figure 6b. To obtain more evidence about the antibacterial efficacy of BUVVH-OH against Gram- negative *E. coli* and Gram- positive *S. aureus* the morphological features of the bacteria were imaged by FE-SEM with and without treatment of BUVVH-OH, as shown in Figure7. Figure 7a shows an SEM image of *E. coli* untreated with gelator that the shows smooth and intact surface of bacterial cell wall. Figure 7b shows an SEM image of *S. aureus* untreated with gelator that reveals no bacterial cell wall collapse and rupture. When the *E. coli* was treated with gelator, BUVVH-OH, morphological alterations including cell wall damage were observed. In this case the cell wall was distorted and some rough and damaged wrinkled cell wall structures are observed. Figure 7c shows an image where some of the damaged cells are indicated by red arrows. Similarly, when the *S. aureus* was treated with the gelator Figure 7d the cells wall was extensively damaged and in some cases, intracellular components were observed leaking out of the cells. This might be due to the lysis of the cell wall of the bacteria. In Fgiure 7d, damaged cells are highlighted with red arrows. Thus, the gelator shows antibacterial activity due to disruption of bacterial cell walls. These observations suggest that the peptide-based hydrogel could have utility asan antibiotic in the near future.
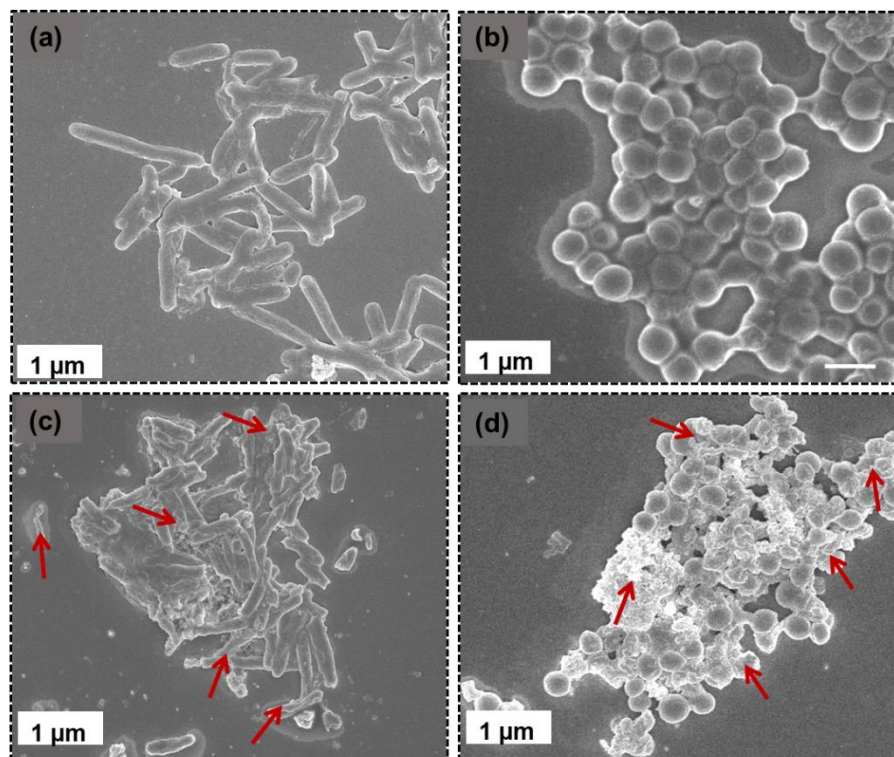
Figure 7. SEM images of (a) *E.coli* and (b) *S. Aureus* before treatment of BUVVH-OH and after treatment of BUVVH-OH for (c) *E.coli* and (d). *S. Aureus.* The red arrows highlighted damaged cell structures.

Drug Release Study: Polymeric hydrogels are widely used for slow release drug delivery applications. However, in some cases polymeric hydrogels show cytotoxicity. Thus supramolecular hydrogels from low molecular weight gelators are of in interest for drug encapsulation and sustainable slow release as these may be non-toxic or less toxic as compared to polymeric gels. Here, the hydrogel obtained from BUVVH-OH, was tested *in vitro* for its ability to show sustained drug release of Naproxen or Doxorubicin. Aliquots 2mg of gelator for

each weres taken and dissolved in 400 µl phosphate buffer. Then, 600 µl solutions of Naproxen or Doxorubicin (0.1 mg) in phosphate buffer were added to the gelator solutions under hot conditions. Each of these drug containing solutions was well shaken and sonicated for homogeneity. It was observed that the solution with Doxorubicin formed a hydrogel during sonication. The solution with Naproxen was kept for 6 min after sonication and it also formed a hydrogel, asconfirmed by vial inversion. Following this, 1ml of buffer solution was carefully layered on top of the surface of each hydrogel to investigate the drug release. The drug release was monitored for 84 h. It was observed that the hydrogel loaded with Doxorubicin showed no release of drug at all. On the other, the hydrogel loaded with Naproxen exhibited a slow and sustained release profile at physiological pH and temperature. In this case the percentage of release of Naproxen was determined by measurement of absorbance using a standard calibration plot obtained from the absorbance of Naproxen of known concentration. The release profile curve (Figure 8) shows that 46% Naproxen is released in the first 9 h. Then the release rate decreasesand the drug is gradually released, 72% of Naproxen being released in 40 h, and 84% over 80 h (Figure 8). Notably, the drug loaded hydrogel was not ruptured over the time of experiment. In the case of Doxorubicin, strong interactions between the the acid group of BUVVH-OH and the amino group of the Doxorubicin may prevent release of the latter from the hydrogel, whereas Naproxen has an acid group that cannot interact with the gelator, enabling release. Figure S7 shows that the storage modulus of hydrogel with Doxorubicin is greater than that of the peptide hydrogel. On the other hand the storage modulus of hydrogel with Naproxen is similar to that of the hydrogel only showing the lack of strong interactions that could hinder release (as with Doxorubicin). These results demonstrate that the hydrogel can be used for the sustainable and slow release of Naproxen at physiological pH and temperature.
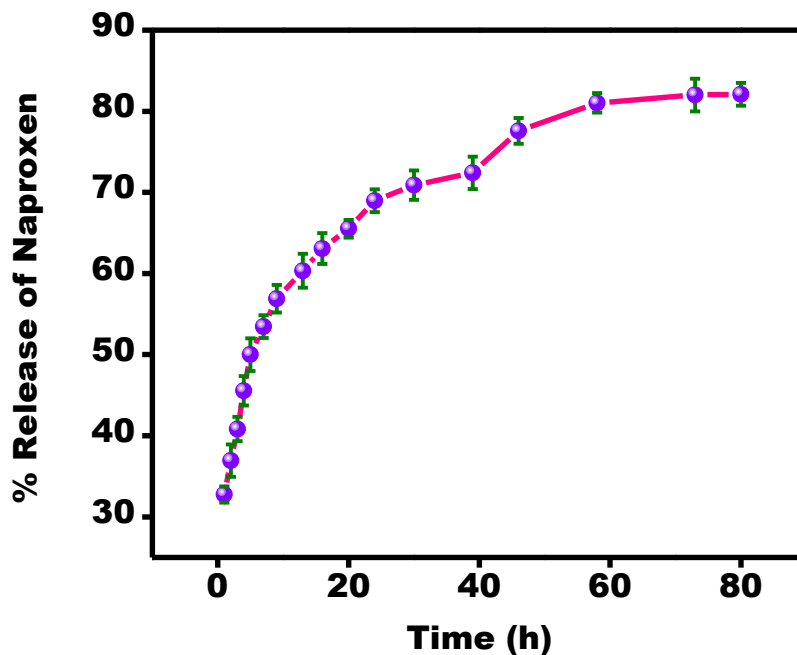
Figure 8. Sustained release of Naproxen from the hydrogel of **P** loaded with 0.1 mg of drug.

Biocompatibility Study:

For practical use in vivo, a gelator must be cytocompatible over a suitable concentration range for which human cells are viable.

Here, different percentage cytotoxicity values are classified as follows: noncytotoxic (>90%), slight (60–90%), moderate (30–60%) and severe (<30%) with respect to control cells cultured in the same medium . The human embryonic kidney (HEK 293T) cell line was used to determine the cytotoxicity of the gelator **P** using an MTT assay. Cell viability was observed after 24 h incubation with different concentrations (0–250μM) of **P**. Under these conditions, it was

observed that the gelator did not show any cytotoxicity to human HEK 293T cells,indicating biocompatibility of the hydrogels (Figure 9).[50]
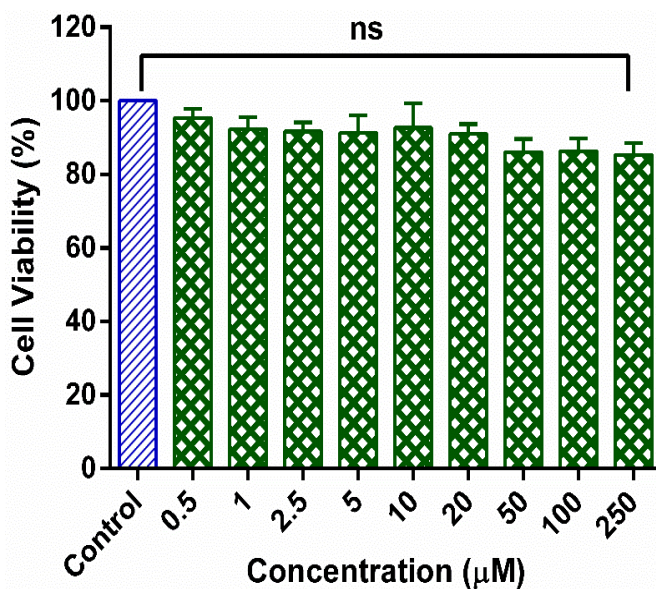

Figure 9. Cell viability of human embryonic kidney (HEK-293) cells after 24 h treatment of different concentrations of the hydrogel as calculated from the MTT assay.

Conclusions

This study demonstrates the preparation and characterization of an injectable, non-cytotoxic histidine- containing peptide- based hydrogel with a stability at the pH range 7.0 to 8.5 in buffer solution. This hydrogel exhibits potent antibacterial activity against both Gram- positive bacteria

(*S. aureus*) and Gram- negative bacteria (*E. coli*) with minimum inhibitory concentration 20-100 µg/ml. Moreover, this hydrogel also exhibits slow and sustained release of Naproxen at physiological condition at pH 7.46 and temperature 37 °C over several days. This hydrogel shows the very interesting property of magnification of images, indicating its lens-like behavior. The controllable drug release, potential antibacterial property and lens-like behavior of this peptide- based non-cytotoxic biomaterial may have future promise for using in health care and materials science.

ASSOCIATED CONTENT

Supporting Information

Experimental details- Synthetic procedure, Spectra of hydrogelator, Magnified image, Thixotropy, Thermal effect, Rheology of drug loaded hydrogel, Proteolytic stability by HRMS.

AUTHOR INFORMATION

Corresponding Author

Arindam Banerjee - School of Biological Sciences, Indian Association for the Cultivation of Science, Jadavpur, Kolkata-700032, India

Email: bcab@iacs.res.in

Authors

Biswanath Hansda - School of Biological Sciences, Indian Association for the Cultivation of Science, Jadavpur, Kolkata 700032, India

Biplab Mondal - School of Biological Sciences, Indian Association for the Cultivation of Science, Jadavpur, Kolkata 700032, India

Jhilam Majumder - Department of Life Science and Biotechnology, Jadavpur University, Jadavpur, Kolkata, 700032, West Bengal, India

Subhadeep Das- Purdue University, 175 South University Street, West Lafayette IN 47907

Sourav Kumar - Department of Biophysics, Bose Institute, Kolkata - 700054

Ratan Gachhui-Department of Life Science and Biotechnology, Jadavpur University, Jadavpur, Kolkata, 700032, West Bengal, India

Ian W. Hamley - School of Chemistry, Pharmacy and Food Biosciences, University of Reading, White knights, Reading, Berkshire RG6 6AD, U.K

Conflict of interest

The authors declare no conflict of interest.

REFERENCES

(1)   Holmes, A. H.; Moore, L. S. P.; Sundsfjord, A.; Steinbakk, M.; Regmi, S.; Karkey, A.; Guerin, P. J.; Piddock, L. J. V. Understanding the Mechanisms and Drivers of Antimicrobial Resistance. *Lancet* **2016**, *387*, 176–187.

(2)   Prestinaci, F.; Pezzotti, P.; Pantosti, A. Antimicrobial Resistance: A Global Multifaceted Phenomenon. *Pathog. Glob. Health* **2015**, *109*, 309–318.

(3)   Wang, W.; Arshad, M. I.; Khurshid, M.; Rasool, M. H.; Nisar, M. A.; Aslam, M. A.; Qamar, M. U. Antibiotic Resistance : A Rundown of a Global Crisis. *Infect. Drug Resist.* **2018**, *11*, 1645–1658.

(4)   Wang, Y.; Garrido-Oter, R.; Wu, J.; Winkelmüller, T. M.; Agler, M.; Colby, T.; Nobori, T.; Kemen, E.; Tsuda, K. Site-Specific Cleavage of Bacterial MucD by Secreted Proteases Mediates Antibacterial Resistance in Arabidopsis. *Nat. Commun.* **2019**, *10*, 2853.

(5)   Willyard, C. The Drug-Resistant Bacteria That Pose the Greatest Health Threats. *Nature* **2017**, *543*, 15.

(6)   Tacconelli, E.; Carrara, E.; Savoldi, A.; Harbarth, S.; Mendelson, M.; Monnet, D. L.; Pulcini, C.; Kahlmeter, G.; Kluytmans, J.; Carmeli, Y.; Ouellette, M.; Outterson, K.; Patel, J.; Cavaleri, M.; Cox, E. M.; Houchens, C. R.; Grayson, M. L.; Hansen, P.; Singh, N.; Theuretzbacher, U.; Magrini, N.; Aboderin, A. O.; Al-Abri, S. S.; Awang Jalil, N.; Benzonana, N.; Bhattacharya, S.; Brink, A. J.; Burkert, F. R.; Cars, O.; Cornaglia, G.; Dyar, O. J.; Friedrich, A. W.; Gales, A. C.; Gandra, S.; Giske, C. G.; Goff, D. A.; Goossens, H.; Gottlieb, T.; Guzman Blanco, M.; Hryniewicz, W.; Kattula, D.; Jinks, T.; Kanj, S. S.; Kerr, L.; Kieny, M. P.; Kim, Y. S.; Kozlov, R. S.; Labarca, J.; Laxminarayan, R.; Leder, K.; Leibovici, L.; Levy-Hara, G.; Littman, J.; Malhotra-Kumar, S.; Manchanda,

V.; Moja, L.; Ndoye, B.; Pan, A.; Paterson, D. L.; Paul, M.; Qiu, H.; Ramon-Pardo, P.; Rodríguez-Baño, J.; Sanguinetti, M.; Sengupta, S.; Sharland, M.; Si-Mehand, M.; Silver, L. L.; Song, W.; Steinbakk, M.; Thomsen, J.; Thwaites, G. E.; van der Meer, J. W.; Van Kinh, N.; Vega, S.; Villegas, M. V.; Wechsler-Fördös, A.; Wertheim, H. F. L.; Wesangula, E.; Woodford, N.; Yilmaz, F. O.; Zorzet, A. Discovery, Research, and Development of New Antibiotics: The WHO Priority List of Antibiotic-Resistant Bacteria and Tuberculosis. *Lancet Infect. Dis.* **2018**, *18*, 318–327.

(7) Babu Rajendran, N.; Mutters, N. T.; Marasca, G.; Conti, M.; Sifakis, F.; Vuong, C.; Voss, A.; Baño, J. R.; Tacconelli, E. Mandatory Surveillance and Outbreaks Reporting of the WHO Priority Pathogens for Research & Discovery of New Antibiotics in European Countries. *Clin. Microbiol. Infect.* **2020**, *26*, 943.e1-943.e6.

(8) Rosen, H.; Abribat, T. The Rise and Rise of Drug Delivery. *Nat. Rev. Drug Discov.* **2005**, *4*, 381–385.

(9) Martí-Centelles, R.; Dolz-Pérez, I.; De la O, J.; Ontoria-Oviedo, I.; Sepúlveda, P.; Nebot, V. J.; Vicent, M. J.; Escuder, B. Two-Component Peptidic Molecular Gels for Topical Drug Delivery of Naproxen. *ACS Appl. Bio Mater.* **2021**, *4*, 935–944.

(10) Nambiar, M.; Schneider, J. P. Peptide Hydrogels for Affinity-Controlled Release of Therapeutic Cargo: Current and Potential Strategies. *J. Pept. Sci.* **2022**, *28*, 1–14.

(11) Heremans, J.; Chevillard, L.; Mannes, M.; Mangialetto, J.; Leroy, K.; White, J. F.; Lamouroux, A.; Vinken, M.; Gardiner, J.; Van Mele, B.; Van den Brande, N.; Hoogenboom, R.; Madder, A.; Caveliers, V.; Mégarbane, B.; Hernot, S.; Ballet, S.; Martin, C. Impact of Doubling Peptide Length on in Vivo Hydrogel Stability and

Sustained Drug Release. *J. Control. Release* **2022**, *350*, 514–524.

(12) Das, A. K.; Gavel, P. K. Low Molecular Weight Self-Assembling Peptide-Based Materials for Cell Culture, Antimicrobial, Anti-Inflammatory, Wound Healing, Anticancer, Drug Delivery, Bioimaging and 3D Bioprinting Applications. *Soft Matter* **2020**, *16*, 10065–10095.

(13) Draper, E. R.; Adams, D. J. Controlling the Assembly and Properties of Low-Molecular-Weight Hydrogelators. *Langmuir* **2019**, *35*, 6506–6521..

(14) Kushner, A. M.; Guan, Z. Modular Design in Natural and Biomimetic Soft Materials. *Angew. Chemie - Int. Ed.* **2011**, *50*, 9026–9057.

(15) Hamley, I. W.; Castelletto, V. Biological Soft Materials. *Angew. Chemie - Int. Ed.* **2007**, *46*, 4442–4455.

(16) Chakraborty, P.; Tang, Y.; Yamamoto, T.; Yao, Y.; Guterman, T.; Zilberzwige-Tal, S.; Adadi, N.; Ji, W.; Dvir, T.; Ramamoorthy, A.; Wei, G.; Gazit, E. Unusual Two-Step Assembly of a Minimalistic Dipeptide-Based Functional Hypergelator. *Adv. Mater.* **2020**, *32*, 1906043.

(17) Abbas, M.; Zou, Q.; Li, S.; Yan, X. Self-Assembled Peptide- and Protein-Based Nanomaterials for Antitumor Photodynamic and Photothermal Therapy. *Adv. Mater.* **2017**, *29*.

(18) Roy, K.; Pandit, G.; Chetia, M.; Sarkar, A. K.; Chowdhuri, S.; Bidkar, A. P.; Chatterjee, S. Peptide Hydrogels as Platforms for Sustained Release of Antimicrobial and Antitumor Drugs and Proteins. *ACS Appl. Bio Mater.* **2020**, *3*, 6251–6262.

(19)   Baral, A.; Roy, S.; Dehsorkhi, A.; Hamley, I. W.; Mohapatra, S.; Ghosh, S.; Banerjee, A. Assembly of an Injectable Noncytotoxic Peptide-Based Hydrogelator for Sustained Release of Drugs. *Langmuir* **2014**, *30*, 929–936.

(20)   De Serres-Bérard, T.; Becher, T. B.; Braga, C. B.; Ornelas, C.; Berthod, F. Neuropeptide Substance P Released from a Nonswellable Laponite-Based Hydrogel Enhances Wound Healing in a Tissue-Engineered Skin in Vitro. *ACS Appl. Polym. Mater.* **2020**, *2*, 5790–5797.

(21)   Tang, J. D.; Mura, C.; Lampe, K. J. Stimuli-Responsive, Pentapeptide, Nanofiber Hydrogel for Tissue Engineering. *J. Am. Chem. Soc.* **2019**, *141*, 4886–4899.

(22)   Bairagi, D.; Biswas, P.; Basu, K.; Hazra, S.; Hermida-Merino, D.; Sinha, D. K.; Hamley, I. W.; Banerjee, A. Self-Assembling Peptide-Based Hydrogel: Regulation of Mechanical Stiffness and Thermal Stability and 3D Cell Culture of Fibroblasts. *ACS Appl. Bio Mater.* **2019**, *2*, 5235–5244.

(23)   DvorÌáková, J.; Trousil, J.; Podhorská, B.; Miks ovská, Z.; Janous ková, O.; Proks, V. Enzymatically Cross-Linked Hydrogels Based on Synthetic Poly(α-Amino Acid)s Functionalized with RGD Peptide for 3D Mesenchymal Stem Cell Culture. *Biomacromolecules* **2021**, *22*, 1417–1431.

(24)   Huang, C. C.; Ravindran, S.; Kang, M.; Cooper, L. F.; George, A. Engineering a Self-Assembling Leucine Zipper Hydrogel System with Function-Specific Motifs for Tissue Regeneration. *ACS Biomater. Sci. Eng.* **2020**, *6*, 2913–2928.

(25)   Baral, A.; Roy, S.; Ghosh, S.; Hermida-Merino, D.; Hamley, I. W.; Banerjee, A. A Peptide-Based Mechano-Sensitive, Proteolytically Stable Hydrogel with Remarkable

Antibacterial Properties. *Langmuir* **2016**, *32*, 1836–1845.

(26) Nandi, N.; Gayen, K.; Ghosh, S.; Bhunia, D.; Kirkham, S.; Sen, S. K.; Ghosh, S.; Hamley, I. W.; Banerjee, A. Amphiphilic Peptide-Based Supramolecular, Noncytotoxic, Stimuli-Responsive Hydrogels with Antibacterial Activity. *Biomacromolecules* **2017**, *18*, 3621–3629.

(27) Gavel, P. K.; Kumar, N.; Parmar, H. S.; Das, A. K. Evaluation of a Peptide-Based Coassembled Nanofibrous and Thixotropic Hydrogel for Dermal Wound Healing. *ACS Appl. Bio Mater.* **2020**, *3*, 3326–3336.

(28) Chowdhuri, S.; Saha, A.; Pramanik, B.; Das, S.; Dowari, P.; Ukil, A.; Das, D. Smart Thixotropic Hydrogels by Disulfide-Linked Short Peptides for Effective Three-Dimensional Cell Proliferation. *Langmuir* **2020**, *36*, 15450–15462..

(29) Lee, T. T.; García, J. R.; Paez, J. I.; Singh, A.; Phelps, E. A.; Weis, S.; Shafiq, Z.; Shekaran, A.; Del Campo, A.; García, A. J. Light-Triggered in Vivo Activation of Adhesive Peptides Regulates Cell Adhesion, Inflammation and Vascularization of Biomaterials. *Nat. Mater.* **2015**, *14*, 352–360.

(30) Mondal, B.; Bairagi, D.; Nandi, N.; Hansda, B.; Das, K. S.; Edwards-Gayle, C. J. C.; Castelletto, V.; Hamley, I. W.; Banerjee, A. Peptide-Based Gel in Environmental Remediation: Removal of Toxic Organic Dyes and Hazardous Pb^{2+} and Cd^{2+} ions from Wastewater and Oil Spill Recovery. *Langmuir* **2020**, *36*, 12942–12953.

(31) Sun, B.; Mi, Z. T.; An, G.; Liu, G.; Zou, J. J. Preparation of Biomimetic Materials Made from Polyaspartyl Polymer and Chitosan for Heavy-Metal Removal. *Ind. Eng. Chem. Res.* **2009**, *48*, 9823–9829.

(32)   Basak, S.; Nanda, J.; Banerjee, A. A New Aromatic Amino Acid Based Organogel for Oil Spill Recovery. *J. Mater. Chem.* **2012**, *22*, 11658–11664.

(33)   Bhattacharya, S.; Krishnan-Ghosh, Y. First Report of Phase Selective Gelation of Oil from Oil/Water Mixtures. Possible Implications toward Containing Oil Spills. *Chem. Commun.* **2001**, 2, 185–186.

(34)   Das, A. K.; Maity, I.; Parmar, H. S.; McDonald, T. O.; Konda, M. Lipase-Catalyzed Dissipative Self-Assembly of a Thixotropic Peptide Bolaamphiphile Hydrogel for Human Umbilical Cord Stem-Cell Proliferation. *Biomacromolecules* **2015**, *16*, 1157–1168.

(35)   Chakraborty, P.; Mondal, S.; Khara, S.; Bairi, P.; Nandi, A. K. Integration of Poly(Ethylene Glycol) in N -Fluorenylmethoxycarbonyl- l -Tryptophan Hydrogel Influencing Mechanical, Thixotropic, and Release Properties. *J. Phys. Chem. B* **2015**, *119*, 5933–5944.

(36)   Kumar, S.; Bajaj, A. Advances in Self-Assembled Injectable Hydrogels for Cancer Therapy. *Biomater. Sci.* **2020**, *8*, 2055–2073.

(37)   Conte, M. P.; Singh, N.; Sasselli, I. R.; Escuder, B.; Ulijn, R. V. Metastable Hydrogels from Aromatic Dipeptides. *Chem. Commun.* **2016**, *52*, 13889–13892.

(38)   Bellotto, O.; Pierri, G.; Rozhin, P.; Polentarutti, M.; Kralj, S.; D'Andrea, P.; Tedesco, C.; Marchesan, S. Dipeptide Self-Assembly into Water-Channels and Gel Biomaterial. *Org. Biomol. Chem.* **2022**, *20*, 6211–6218.

(39)   Thota, C. K.; Mikolajczak, D. J.; Roth, C.; Koksch, B. Enhancing Antimicrobial Peptide Potency through Multivalent Presentation on Coiled-Coil Nanofibrils. *ACS Med. Chem.*

Lett. **2021**, *12*, 67–73.

(40)   Wang, S. H.; Tang, T. W. H.; Wu, E.; Wang, D. W.; Liao, Y. Di. Anionic Surfactant-Facilitated Coating of Antimicrobial Peptide and Antibiotic Reduces Biomaterial-Associated Infection. *ACS Biomater. Sci. Eng.* **2020**, *6*, 4561–4572.

(41)   Castelletto, V.; Hamley, I. W. Amyloid and Hydrogel Formation of a Peptide Sequence from a Coronavirus Spike Protein. *ACS Nano* **2022**, *16*, 1857–1867.

(42)   Pelin, J. N. B. D.; Gerbelli, B. B.; Edwards-Gayle, C. J. C.; Aguilar, A. M.; Castelletto, V.; Hamley, I. W.; Alves, W. A. Amyloid Peptide Mixtures: Self-Assembly, Hydrogelation, Nematic Ordering, and Catalysts in Aldol Reactions. *Langmuir* **2020**, *36*, 2767–2774.

(43)   Zhu, H.; Mei, X.; He, Y.; Mao, H.; Tang, W.; Liu, R.; Yang, J.; Luo, K.; Gu, Z.; Zhou, L. Fast and High Strength Soft Tissue Bioadhesives Based on a Peptide Dendrimer with Antimicrobial Properties and Hemostatic Ability. *ACS Appl. Mater. Interfaces* **2020**, *12*, 4241–4253.

(44)   Sambhy, V.; Peterson, B. R.; Sen, A. Antibacterial and Hemolytic Activities of Pyridinium Polymers as a Function of the Spatial Relationship between the Positive Charge and the Pendant Alkyl Tail. *Angew. Chem. Int. Ed. Engl.* **2008**, *47*, 1250–1254.

(45)   Das, D.; Maiti, S.; Brahmachari, S.; Das, P. K. Refining Hydrogelator Design: Soft Materials with Improved Gelation Ability, Biocompatibility and Matrix for in Situ Synthesis of Specific Shaped GNP. *Soft Matter* **2011**, *7* , 7291–7303.

(46)   Nanda, J.; Banerjee, A. β-Amino Acid Containing Proteolitically Stable Dipeptide Based

Hydrogels: Encapsulation and Sustained Release of Some Important Biomolecules at Physiological PH and Temperature. *Soft Matter* **2012**, *8*, 3380–3386.

(47) Yang, Z.; Liang, G.; Xu, B. Supramolecular Hydrogels Based on β-Amino Acid Derivatives. *Chem. Commun.* **2006**, 7, 738–740.

(48) Xu, F.; Padhy, H.; Al-Dossary, M.; Zhang, G.; Behzad, A. R.; Stingl, U.; Rothenberger, A. Synthesis and Properties of the Metallo-Supramolecular Polymer Hydrogel Poly[Methyl Vinyl Ether-Alt-Mono-Sodium Maleate]·AgNO3: Ag^+/Cu^{2+} Ion Exchange and Effective Antibacterial Activity. *J. Mater. Chem. B* **2014**, *2*, 6406–6411.

(49) Yang, K.; Han, Q.; Chen, B.; Zheng, Y.; Zhang, K.; Li, Q.; Wang, J. Antimicrobial Hydrogels: Promising Materials for Medical Application. *Int. J. Nanomedicine* **2018**, *13*, 2217–2263.

(50) Rai, Y.; Pathak, R.; Kumari, N.; Sah, D. K.; Pandey, S.; Kalra, N.; Soni, R.; Dwarakanath, B. S.; Bhatt, A. N. Mitochondrial Biogenesis and Metabolic Hyperactivation Limits the Application of MTT Assay in the Estimation of Radiation Induced Growth Inhibition. *Sci. Rep.* **2018**, *8*, 1–15.

Amphiphilic peptide based gelator formed hydrogel in phosphate buffer. It showed potent antibacterial activitly against Gram positive (*S. aureus*) and Gram negative bacteria (*E. coli*).The hydrogel also exhibited efficacy of slow and sustain release of Naproxen.

TABLE OF CONTENTs

Histidine- Containing Amphiphilic Peptide- Based Non-cytotoxic Hydrogelator with Antibacterial Activity and Sustainable Drug Release

(1)
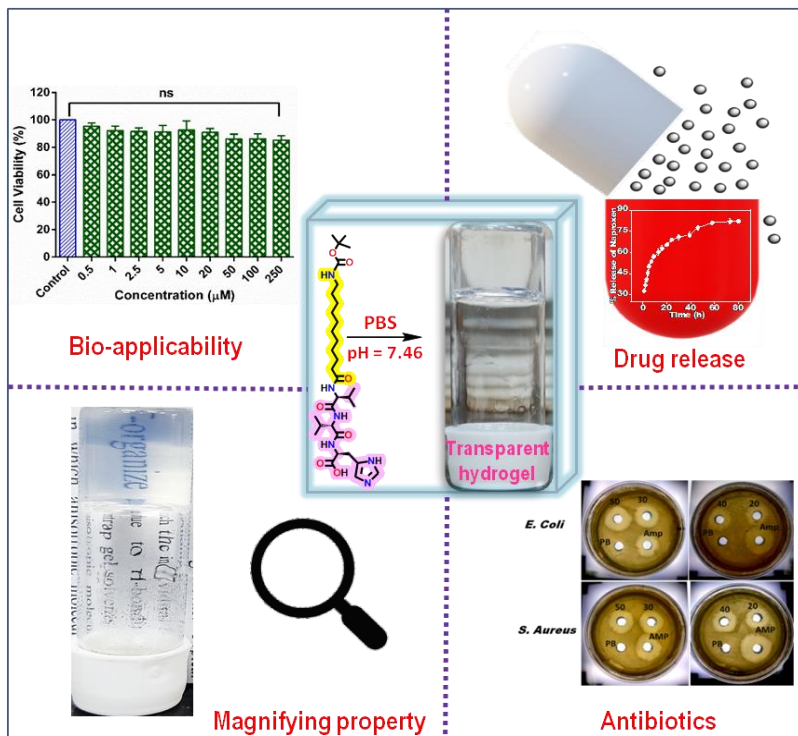
Cowieson, N. P.; Edwards-Gayle, C. J. C.; Inoue, K.; Khunti, N. S.; Doutch, J.; Williams, E.; Daniels, S.; Preece, G.; Krumpa, N. A.; Sutter, J. P.; Tully, M. D.; Terrill, N. J.; Rambo, R. P., Beamline B21: high-throughput small-angle X-ray scattering at Diamond Light Source. *Journal of Synchrotron Radiation* **2020,** *27*, 1438-1446.

(2)   Edwards-Gayle, C. J. C.; Khunti, N.; Hamley, I. W.; Inoue, K.; Cowieson, N.; Rambo, R., Design of a multipurpose sample cell holder for the Diamond Light Source high-throughput SAXS beamline B21. *Journal of Synchrotron Radiation* **2021,** *28*, 318-321.